Cardiovascular Research (2016) **110**, 30–39
doi:10.1093/cvr/cvw014

Modulators of right ventricular apoptosis and contractility in a rat model of pulmonary hypertension

Makhosazane Zungu-Edmondson, Nataliia V. Shults, Chi-Ming Wong, and Yuichiro J. Suzuki*

Department of Pharmacology and Physiology, Georgetown University Medical Center, 3900 Reservoir Road NW, Washington DC 20057, USA

Received 8 October 2015; revised 24 December 2015; accepted 30 December 2015; online publish-ahead-of-print 19 January 2016

Time for primary review: 36 days

Aims Right ventricular (RV) failure is the major cause of death among patients with pulmonary arterial hypertension (PAH). However, the mechanism of RV failure has not been defined.

Methods and results This study examined mechanisms and consequences of RV myocyte apoptosis and fibrosis in response to PAH. Rats were injected with SU5416 (vascular endothelial growth factor inhibitor), followed by hypoxia for 3 weeks, and subsequently maintained in normoxia for 2, 5, or 14 weeks (5-, 8-, and 17-week time points after the SU5416 injection, respectively). RV systolic pressure (RVSP) was elevated to >70 mmHg at 5-week time point, and this pressure was sustained thereafter. Significant RV myocyte apoptosis and fibrosis were observed at 8- and 17-week time points. Apoptosis was associated with downregulated Bcl-x_L (anti-apoptotic protein), downregulated GATA4 (transcriptional regulator of Bcl-x_L), and upregulated p53 (negative regulator of GATA4 gene transcription). PAH-mediated RV apoptosis and fibrosis were attenuated in p53 knock-out rats. Despite the major loss of cardiomyocytes, RV contractility was enhanced, suggesting that the remaining myocytes can perform improved contractile functions. Improved RV contractility is associated with the increased expression of contractile and sarcoplasmic reticulum Ca^{2+} uptake proteins. In contrast, the expression of calsequestrin 2 (CSQ2) was downregulated. The siRNA knockdown of CSQ2 improved RV contractility and increased the expression of contractile and Ca^{2+} uptake proteins.

Conclusion These results suggest that RV decompensation is associated with the death of cardiomyocytes, resulting in fibrosis. However, the remaining myocytes are capable of sustaining RV contractility through the mechanism that involves CSQ2.

Keywords Calsequestrin • Hypertrophy • p53 • Pulmonary hypertension • Right ventricle • Right ventricular failure

1. Introduction

Pulmonary arterial hypertension (PAH) can occur without known causes or secondary to other diseases such as various lung diseases including chronic obstructive pulmonary disease and interstitial lung disease.[1] Despite the availability of FDA-approved treatment options, PAH remains a fatal disease with a poor prognosis (3-year survival rate is only 58–75%).[2–4] The initial response to chronic pulmonary arterial pressure overload is the enlargement of the right ventricular (RV) wall to obtain a stronger force of muscle contraction. This initial compensatory activity, however, ultimately transitions to heart failure, and right heart failure is the major cause of death among patients with PAH.[5]

The apparent mechanisms of heart failure in the right and left sides of the heart, in response to pulmonary and systemic hypertensions, respectively, are different. Concentric hypertrophy of the left ventricle (LV) transitions to LV dilation with the thinning of LV walls. In contrast, the classical property of the failed RV in cor pulmonale is the concentrically hypertrophied RV.[6,7] It is unclear whether therapeutic agents that are designed to treat LV dysfunction provide benefits to the RV because RV pathophysiology has not been well defined.[8]

In response to chronic pressure overload, the heart adapts by increasing the cardiomyocyte size to increase the force of contraction. The development of cardiac hypertrophy is associated with various qualitative and quantitative changes in the myocardium. One important

* Corresponding author. Tel: +1 202 687 8090; fax: +1 202 687 8825, Email: ys82@georgetown.edu

event that occurs in the hypertrophied heart is angiogenesis, the formation of new coronary vessels by sprouting from preexisting vessels. Pressure overload ultimately results in a mismatch between capillary density and the size of individual cardiomyocytes, leading to myocardial hypoxia.[9] RV ischaemia has been observed in the hearts of PAH patients with normal coronary arteries as a consequence of increased oxygen demand and a loss of RV microvessels.[10]

The chronic hypoxia model of pulmonary hypertension has been well used to study RV hypertrophy. However, this model does not cause right heart failure. The combined use of vascular endothelial growth factor (VEGF) receptor inhibitor, SU5416, and hypoxia in rats leads to vascular alterations similar to those observed in human patients with severe PAH.[11,12] This model also shows signs of RV failure including the occurrence of cardiomyocyte apoptosis and cardiac fibrosis, presumably due to the inhibition of angiogenesis.[13]

This study uses an SU5416/hypoxia model to further determine the mechanisms and consequences of RV alterations in response to severe PAH and the lack of angiogenesis.

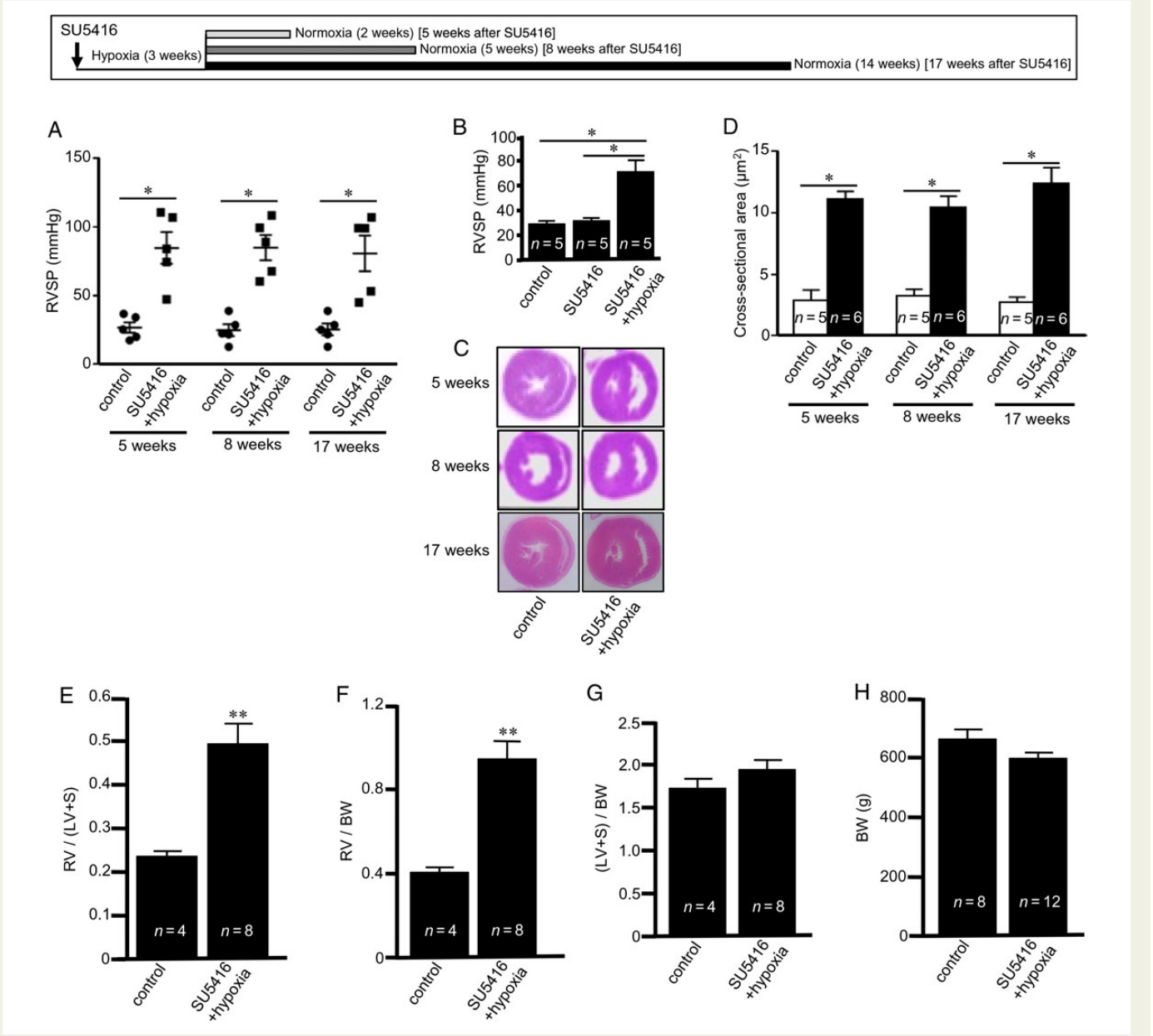

Figure 1 PAH induces pulmonary hypertension and RV hypertrophy. SU5416-injected rats were subjected to 3 weeks hypoxia and then maintained in normoxia for 2, 5, or 14 weeks (5-, 8-, and 17-week time points, respectively). (*A*) RVSP was monitored using a Millar catheter; (*B*) RVSP at 5 weeks after SU5416 injection; (*C*) H&E staining showing the thickened RV wall; (*D*) RV myocyte cross-sectional area; (*E*) RV, LV, and septum were weighed and Fulton's index was calculated as an indication of RV hypertrophy; (*F*) the ratio of RV weight to body weight (BW); (*G*) the ratio of LV + septum weight to BW; and (*H*) BW. Results in (*E*–*H*) are from 8-week time point. The symbol (*) denotes that the values are significantly different from each other at $P < 0.05$ as determined by one-way ANOVA. The symbol (**) indicates that the value is significantly different from the control value at $P < 0.05$ as determined by Student's *t*-test.

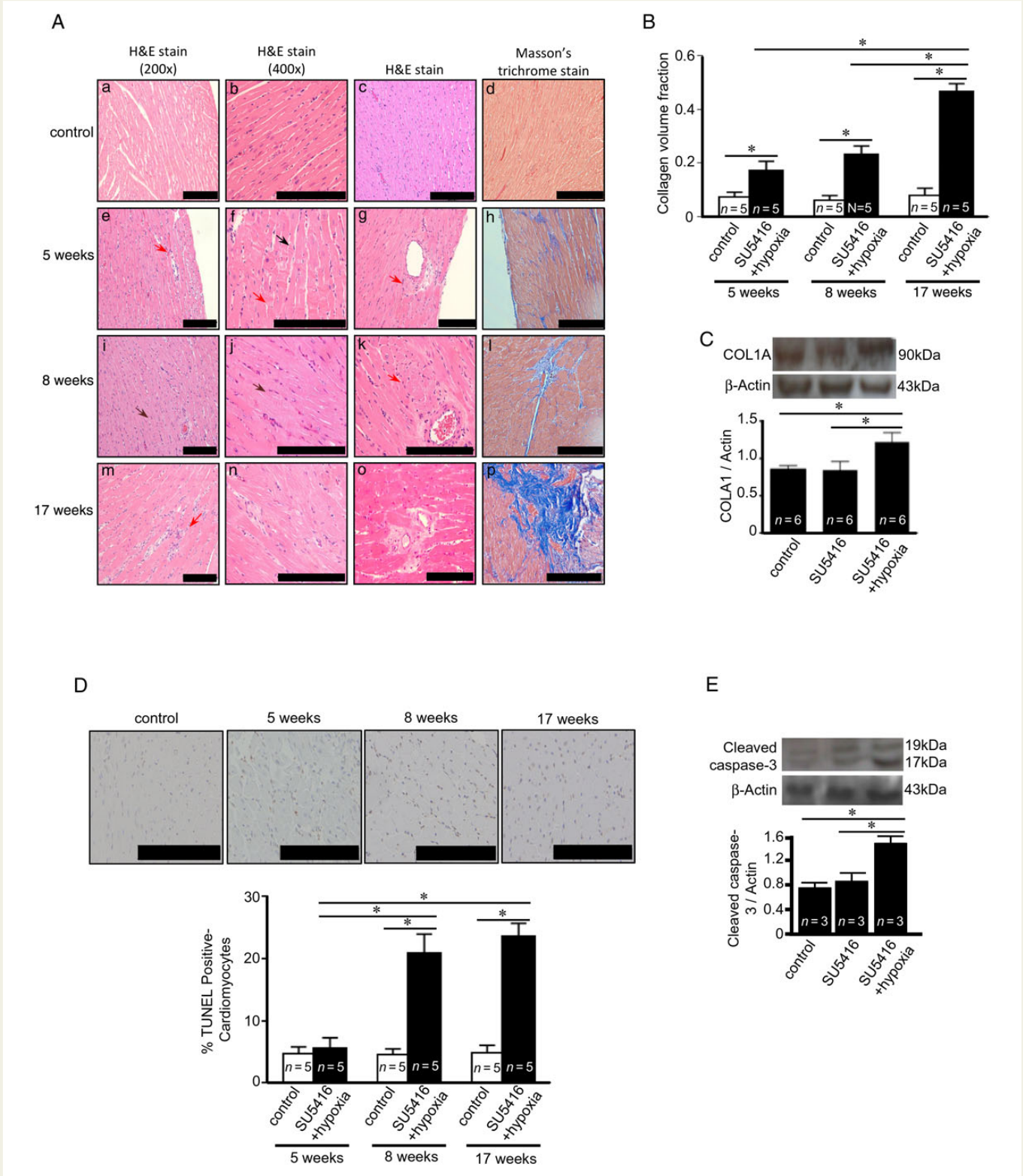

Figure 2 PAH causes apoptosis and fibrosis in the RV. Rats were subjected to SU5416/hypoxia followed by 2, 5, or 14 weeks of normoxia (5-, 8-, and 17-time points, respectively). (*A*) H&E stain images from two different magnifications. H&E staining of the perivascular region is also shown. Masson's trichrome stain with collagen stained in blue with 200× magnification. (*B*) Quantification of Masson's trichrome stain detecting collagen volume fraction. (*C*) Western blotting showing increased collagen type 1a (COLA1) in the RV at 8 weeks after the SU5416 injection. (*D*) TUNEL assays were performed and percentage of apoptotic cardiomyocytes was determined. (*E*) Western blotting showing increased cleaved caspase-3 at 8 weeks after the SU5416 injection. The symbol (*) denotes that the values are significantly different from each other at $P < 0.05$ as determined by one-way ANOVA. Results presented in (*B*) and (*D*) were also analysed using two-way ANOVA. Scale bars, 200 μm.

2. Methods

2.1 Animal treatment

Male Sprague–Dawley rats (~250 g; Charles River Laboratories International, Inc., Wilmington, MA, USA) were subcutaneously injected with 20 mg/kg body weight SU5416 (TOCRIS, Minneapolis, MN, USA) dissolved in carboxymethylcellulose sodium, sodium chloride, polysorbate 80, benzyl alcohol, and dimethyl sulphoxide and maintained in hypoxia for 3 weeks and then in normoxia for 2, 5, or 14 weeks (designated as 5-, 8-, and 17-week time points, respectively).[11,12] Animals were subjected to hypoxia in a chamber (30″ w × 20″ d × 20″ h) regulated by an OxyCycler Oxygen Profile Controller (Model A84XOV; BioSpherix, Redfield, NY, USA) that was set to maintain 10% O_2 with an influx of nitrogen gas, located in the animal care facility at Georgetown University Medical Center.[14] Ventilation to the outside of the chamber was adjusted to remove CO_2, such that its level did not exceed 5000 ppm. Control animals were injected with saline and subjected to ambient 21% O_2 (normoxia) in another chamber. Animals were fed normal rat chow during the treatment. For some experiments, p53 knock-out rats with the Sprague–Dawley background that were purchased from SAGE Labs (Boyertown, PA, USA) were used.

At the end of the experiments, some rats were anaesthetized with intraperitoneal injections of xylazine (10 mg/kg body weight) and ketamine (100 mg/kg body weight). They were then intubated and mechanically ventilated with a volume-controlled Inspira Advanced Safety Ventilator (Harvard Apparatus, Holliston, MA, USA). Rats were maintained on a heat pad, and the temperature was kept at 37°C by using a TR-200 Temperature Controller connected to a rectal probe (Fine Scientific Tools, North Vancouver, Canada). After a thoracotomy through the third left intercostal space, a Millar catheter (1.4 F) was inserted into the RV. RV pressure signals were recorded by using PowerLab with Chart 5 software (ADInstruments, Colorado Springs, CO, USA).

For the *in vivo* siRNA to knockdown cardiac calsequestrin 2 (CSQ2), male Sprague–Dawley rats (~50 g) were injected with 100 μg Ambion *In Vivo* Pre-Designed siRNA for Casq2 (ID: s130916; Life Technologies, Carlsbad, CA, USA) and 50 μL Nanoparticle *In Vivo* Transfection Reagent (Altogen Biosystems, Las Vegas, NV, USA) by using the tail vein systemic intravenous (i.v.) injection method. After 48 h, rats were anaesthetized with an intraperitoneal injection of urethane (1.5 mg/kg body weight).

The Georgetown University Animal Care and Use Committee approved all animal experiments (Protocol Number 13-044-100109), and the investigation conforms to the National Institutes of Health Guide for the Care and Use of Laboratory Animals.

2.2 Histological measurements

Heart tissues were immersed in buffered 10% paraformaldehyde at room temperature and were embedded in paraffin. Paraffin-embedded tissues were cut and mounted on glass slides. Tissue sections were stained with haematoxylin and eosin (H&E). Tissue sections were also evaluated for the occurrence of apoptosis by terminal deoxynucleotidyl transferase dUTP nick end labelling (TUNEL) assay using the ApopTag Peroxidase *In Situ* Apoptosis Detection Kit (EMD Millipore, Billerica, MA, USA) and for the occurrence of fibrosis by Masson's trichrome stain.[14] For quantifications of histological specimen, slides were blinded and the RV free wall was analysed microscopically using 20× magnification on a IX71 Microscope (Olympus, Center Valley, PA, USA) and the ImageJ software (NIH). % TUNEL-positive cardiomyocytes were calculated by assessing the number of apoptotic cells (brown stain) and the number of total cardiomyocyte nuclei (blue stain). The collagen volume fraction as an indication of fibrosis was calculated by measuring the blue areas of Masson's trichrome-stained slides. Eight different fields were examined for each animal.

2.3 Immunoblotting analysis

RVs were homogenized and protein gel electrophoresis samples were prepared as described previously.[14,15] For immunoblotting, equal protein amounts of samples were electrophoresed through a reducing sodium dodecyl sulphate–polyacrylamide gel and electroblotted onto a membrane. The membrane was blocked and incubated with antibodies for cleaved caspase-3 (Cell Signaling Technology, Inc., Danvers, MA, USA), collagen A1, Bcl-x_L, GATA4, p53, tropomyosin, troponin T, SERCA2, triadin (Santa Cruz Biotechnology, Inc., Dallas, TX, USA), and CSQ2 (EMD Millipore), and levels of proteins were detected by using horseradish peroxidase-linked secondary antibodies and an Enhanced Chemiluminescence System (GE Healthcare Bio-Sciences, Pittsburgh, PA, USA).

2.4 Statistical analysis

Means and standard errors were calculated. Comparisons between two groups were analysed by using a two-tailed Student's *t*-test, and comparisons among three or more groups were analysed by using one- or two-way analysis of variance (ANOVA) with a Student–Newman–Keuls *post hoc* test using GraphPad Prism (GraphPad Software, Inc., La Jolla, CA, USA), in accordance with the Kolmogorov–Smirnov test for normality. $P < 0.05$ was considered to be significant.

3. Results

3.1 SU5416/hypoxia treatment induces RV hypertrophy, apoptosis, and fibrosis

The subcutaneous injection of SU5416, exposure to chronic hypoxia (10%, O_2) for 3 weeks, and subsequent maintenance of animals in

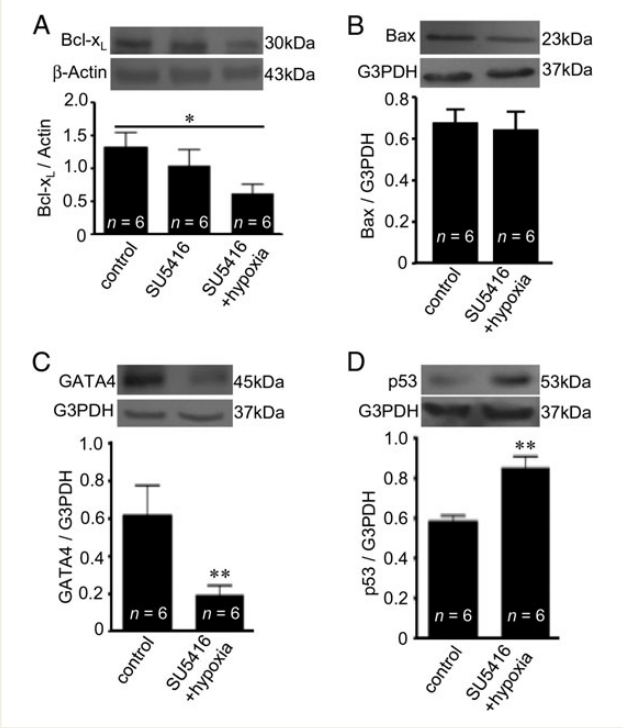

Figure 3 PAH decreases gene expression of anti-apoptotic Bcl-x_L in the RV. Rats were subjected to SU5416/hypoxia treatment (8-week time point). Protein expression of (*A*) Bcl-x_L, (*B*) Bax, (*C*) GATA4, and (*D*) p53 were monitored by western blotting in the RV. The symbol (*) denotes that the values are significantly different from each other at $P < 0.05$ as determined by one-way ANOVA. The symbol (**) indicates that the value is significantly different from the control value at $P < 0.05$ as determined by Student's *t*-test.

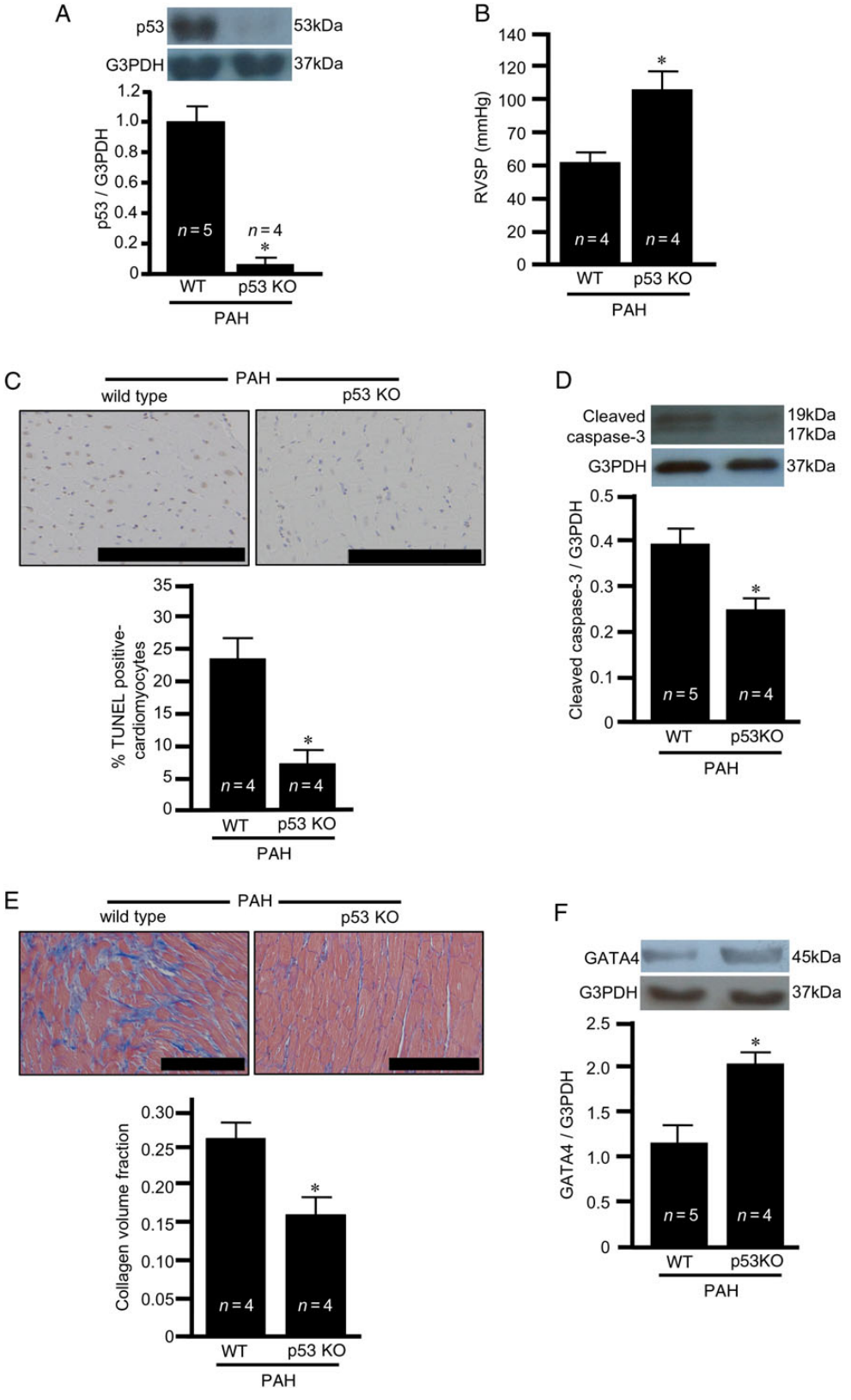

Figure 4 PAH-induced apoptosis and fibrosis in the RV are p53-dependent. Wild-type (WT) and p53 knock-out (KO) rats were subjected to the SU5416 injection, hypoxia for 3 weeks, and maintained for 5 weeks in normoxia (8-week time point). (*A*) Western blotting showing the p53 level in the RV; (*B*) RVSP; (*C*) TUNEL-positive RV myocytes (brown stain); (*D*) cleaved caspase-3 levels in the RV as monitored by western blotting; (*E*) Masson's trichrome stain to monitor fibrosis (blue stain) in the RV; and (*F*) GATA4 expression in the RV. The symbol (*) denotes that the value is significantly different from the WT value at $P < 0.05$ as determined by Student's *t*-test. Scale bars, 200 μm.

normoxia resulted in the development of PAH with elevated RVSP (*Figure 1A*). SU5416 alone without hypoxia did not increase RV pressure (*Figure 1B*). RV hypertrophy was apparent in these pulmonary hypertensive animals as indicated by the increased RV wall thickness in H&E-stained histological specimens (*Figure 1C*), increased RV myocyte cross-sectional areas (*Figure 1D*), increased Fulton's index, RV/(LV + septum) weights (*Figure 1E*), and RV weight over body weight (*Figure 1F*). In contrast, LV + septum weight over body weight did not change (*Figure 1G*). Further, no changes in body weight were noted (*Figure 1H*). Almost 25% of the rats died during the first 5 weeks of SU5416 injection, and 10% of rats died between 5- and 17-week time points (see Supplementary material online, *Figure S1*).

Histological examinations of H&E-stained RV tissue sections from rats with PAH as shown in *Figure 2A* revealed dramatic changes in myocardial structure of the RV subjected to PAH. The RV from healthy control animals exhibited the syncytium of myocardial fibres with central nuclei. Faint pink intercalated discs are seen joining cardiomyocytes. In contrast, the RVs from SU5416/hypoxia-treated rats suffer from myocyte degeneration, polymorphic cardiomyocytes, and myofibre disarray. As early as at 5-week time point, H&E stain shows the occurrence of contractures of cardiomyocytes (black arrow in *Figure 2A-f*), hyperbasophilia, hypereosinophilia, wavy arrangement of myofibres (brown arrows in *Figure 2A-i* and *-j*), myocytolysis (red arrows in *Figure 2A-e–g*, *-k*, and *-m*), loss of myofibril striations, cell oedema, and lesions and death of cardiomyocytes.

The RV from the PAH animals also suffered from significant levels of replacement fibrosis. In H&E-stained RV tissues, perivascular fibrosis was observed in the RV of rats treated with SU5416/hypoxia at all the time points (*Figure 2A*). Masson's trichrome stain shows the induction of perivascular and focal myocardial fibrosis visualized in blue (*Figure 2A*). By 17-week time point, 50% of the RV area was found to be fibrotic (*Figure 2B*). Immunoblotting for collagen A1 confirmed the increased fibrosis in the RV (*Figure 2C*).

TUNEL staining showed the increase in apoptotic myocytes in the RV (*Figure 2D*), but not in the LV (data not shown). A statistically significant increase in RV myocyte apoptosis was observed 8 and 17 weeks after the injection of SU5416. The occurrence of apoptosis was confirmed by monitoring the expression of cleaved caspase-3 by immunoblotting (*Figure 2E*).

These deleterious changes in RV myocytes were associated with decreased expression of endothelial cell marker PECAM-1 (platelet/endothelial cell adhesion molecule-1), indicating reduced angiogenesis (see Supplementary material online, *Figure S2*).

3.2 Mechanism of RV myocyte apoptosis

Apoptosis can be promoted as a result of the downregulation of anti-apoptotic proteins such as Bcl-x_L. Consistently, we found that SU5416/hypoxia-treated rats have a downregulated expression of Bcl-x_L in the RV (*Figure 3A*). The SU5416 administration alone without hypoxia had no effects (*Figure 3A*). In contrast, we did not observe any changes in the expression of pro-apoptotic Bax (*Figure 3B*). Bcl-x_L expression is regulated by a transcription factor GATA4,[16] and the GATA4 expression was found to be reduced in the RV of SU5416/hypoxia-treated rats (*Figure 3C*). We have previously reported that GATA4 gene transcription is negatively regulated by p53,[17] and SU5416/hypoxia-treated rats were found to have increased p53 in the RV (*Figure 3D*). These results are consistent with the model, in which the p53 activation promotes RV myocyte apoptosis.

To directly test this hypothesis, we employed p53 knock-out rats. Immunoblotting showed that p53 was indeed absent in these knock-out rats (*Figure 4A*). The treatment of p53 knock-out rats enhanced the development of pulmonary hypertension, as shown by monitoring RV pressure (*Figure 4B*). The degrees of compensatory RV hypertrophy induced by PAH were similar between wild-type and p53 knock-out rats as determined by Fulton's index (see Supplementary material online, *Figure S3A*) where the heart weights are not different (*Figure S3B*) and RV weight divided by body weight (*Figure S3C*) where the body weights are not different (*Figure S3D*). Despite exaggerated pulmonary hypertension and the occurrence of RV hypertrophy, p53 knock-out rats were found to have reduced RV myocyte apoptosis (*Figure 4C* and *D*) and fibrosis (*Figure 4E*) in response to SU5416/hypoxia-induced PAH. These results suggest the involvement of p53 in PAH-induced RV myocyte apoptosis and fibrosis that occur during RV decompensation. The GATA4 expression that is reduced by SU5416/hypoxia treatment was restored in p53 knock-out rats (*Figure 4F*), supporting our hypothesis that the negative regulation of GATA4 gene transcription by p53 promotes apoptosis.

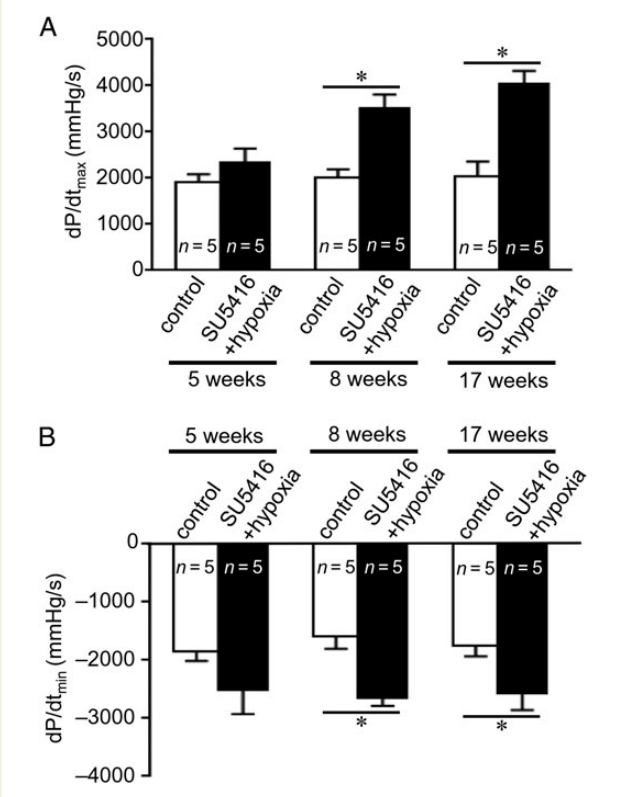

Figure 5 RV contractility is maintained despite the occurrence of apoptosis and fibrosis. Rats were subjected to SU5416 injection, hypoxia for 3 weeks, and maintained for 2, 5, or 14 weeks in normoxia (5-, 8-, and 17-week time points). Rats were ventilated and the chest opened. A Miller catheter was inserted into the RV apex, and (*A*) dP/dt_{max} and (*B*) dP/dt_{min} values were measured as an indication of the contractile performance. The symbol (*) indicates that the values are significantly different from each other at $P < 0.05$ as determined by one-way ANOVA.

3.3 Contractile function is maintained in the apoptotic/fibrotic RV

Remarkably, despite pronounced apoptosis and fibrosis, the RV from rats treated with SU5416/hypoxia was found to have enhanced cardiac contractile functions as assessed by dP/dt_{max} and dP/dt_{min} (*Figure 5*). Although RV pressure sustained at a similar level for 5, 8, and 17 weeks after the SU5416 injection, dP/dt progressively increased. These results suggest that the RV is capable of generating a higher contractile force with a smaller number of cardiomyocytes.

Although total muscle protein levels were reduced in the RV affected by SU5416/hypoxia-mediated PAH, the expression levels of contractive proteins such as tropomyosin (*Figure 6A*) and troponin T (*Figure 6B*) were elevated. This increase in contractile proteins may contribute to the higher force of contraction by the RV affected by PAH. Similarly, the expression level of sarcoplasmic reticulum (SR) Ca^{2+}-ATPase (SERCA2), the major Ca^{2+} uptake protein of the SR, was found to be increased (*Figure 6C*), indicating that the remaining RV myocytes are capable of having a higher Ca^{2+} store in the SR. In contrast, interestingly, cardiac CSQ2, the major Ca^{2+}-binding protein within the SR (*Figure 6D*), and its associated protein triadin (*Figure 6E*) were found to be downregulated in the RV affected by PAH.

To test the hypothesis that the reduction of CSQ2 may be involved in the creation of RV myocytes with improved contractile functions, CSQ2 was knocked down in rats. By using stable siRNA designed for *in vivo* use and a nanoparticle-based transfection reagent, the CSQ2 expression level was successfully reduced in the RV (*Figure 7A*). RV contractility, as measured by dP/dt_{max}, was found to be increased in animals with a reduced CSQ2 expression in the RV (*Figure 7B*), supporting the hypothesis that the downregulation of CSQ2 is a means to increase RV contractility.

The link between CSQ2 and the expression of contractile and Ca^{2+} uptake proteins was studied in rats with CSQ2 knocked down by siRNA. We found that the expression levels of all the proteins that are upregulated in response to PAH in the RV including tropomyosin (*Figure 7C*), troponin T (*Figure 7D*), and SERCA2 (*Figure 7E*) were enhanced by the CSQ knockdown.

4. Discussion

PAH is characterized by increased pulmonary arterial pressure, resulting in increased RV afterload and subsequent right heat failure. The SU5416/hypoxia model provides a unique and useful tool for studying PAH and RV failure. This model develops severe PAH whose vascular pathology closely resembles clinical PAH, and the lack of angiogenesis due to the inhibition of VEGF appears to promote RV decompensation.[1,13,18] As chronic pulmonary arterial pressure elevation by

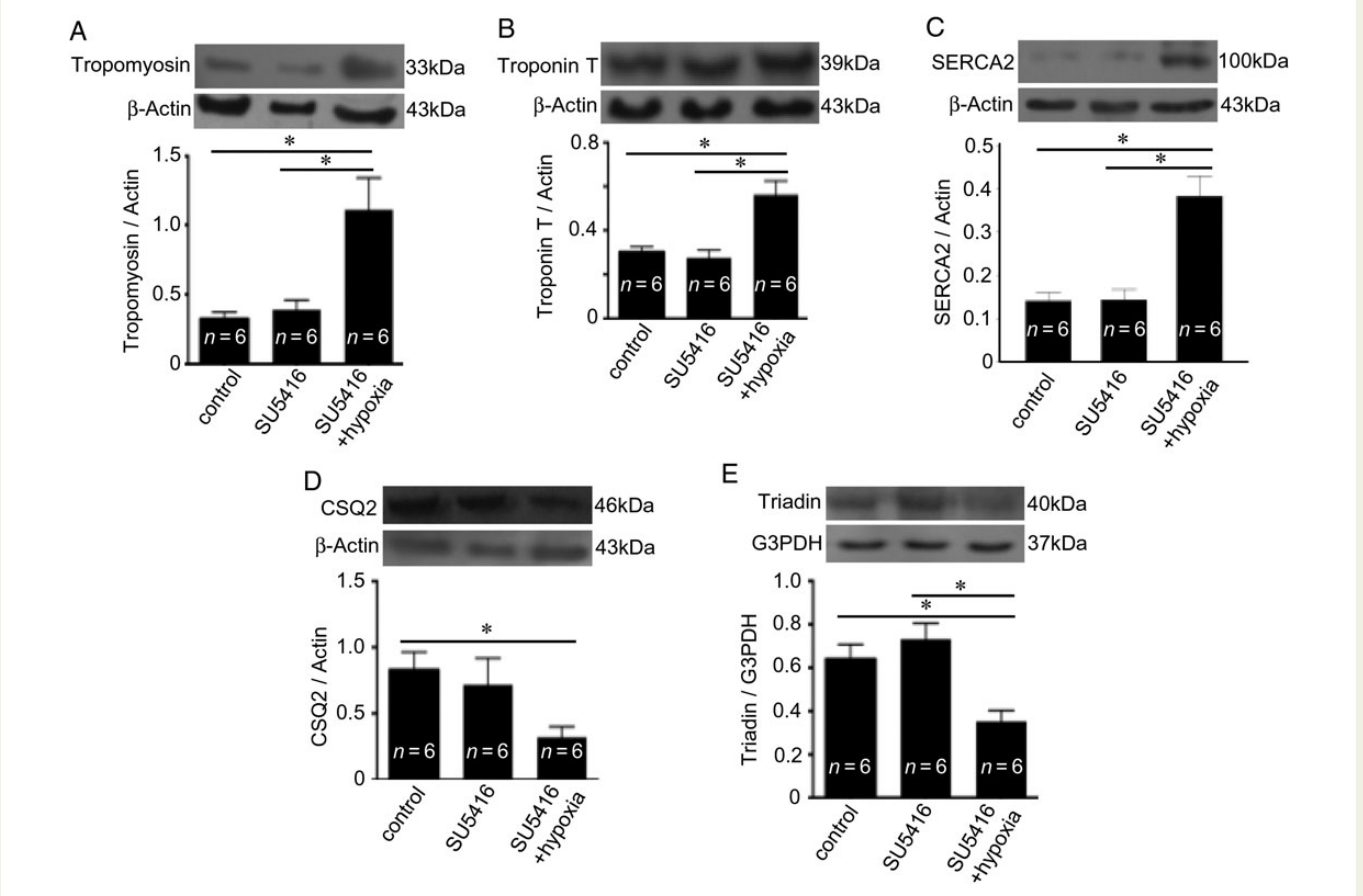

Figure 6 PAH upregulates the expression of contractile and SR uptake proteins, but downregulates CSQ2, in the RV. Rats were subjected to SU5416/hypoxia treatment (8-week time point). (*A*) Tropomyosin, (*B*) troponin T, (*C*) SERCA2a, (*D*) CSQ2, and (*E*) triadin levels were monitored by western blotting in the RV homogenates. The symbol (*) denotes that the values are significantly different from each other at $P < 0.05$ as determined by one-way ANOVA.

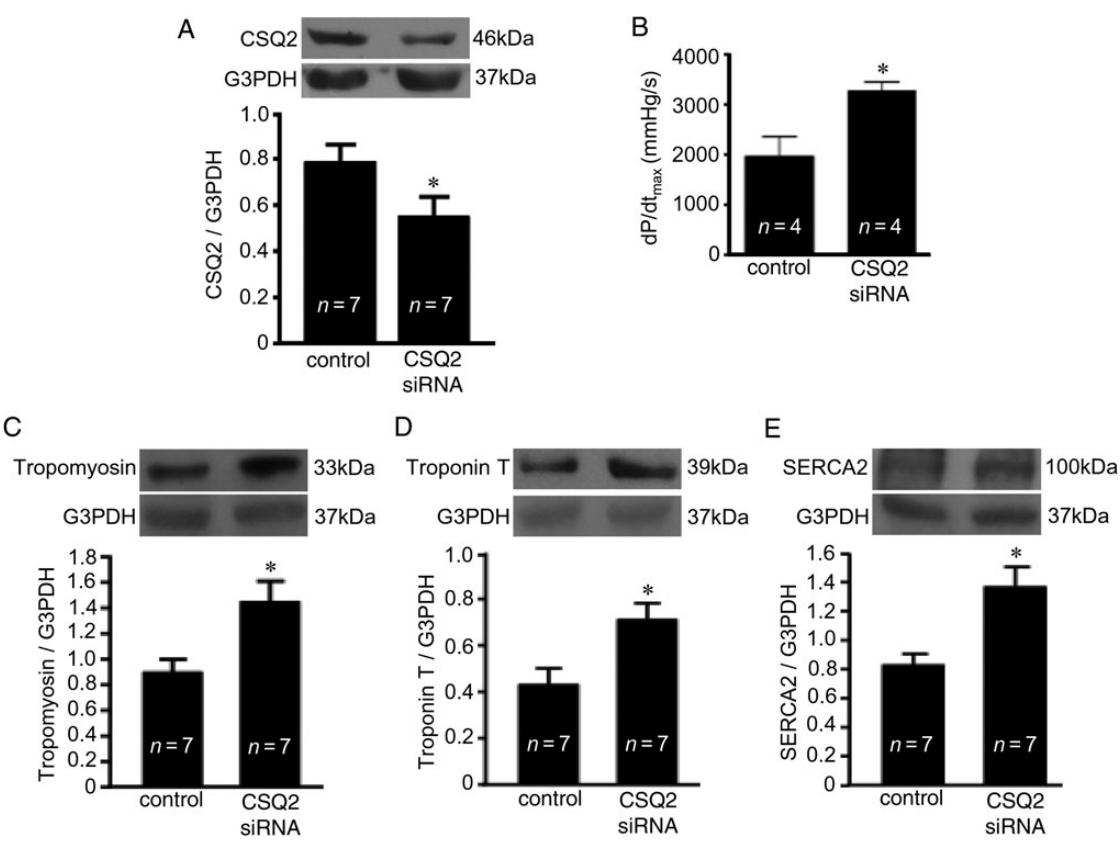

Figure 7 CSQ2 knockdown in the RV mimics the effects of PAH. Rats were treated with *in vivo* siRNA for 48 h to knockdown CSQ2, and the Millar catheter was used to measure RV contractile functions. (*A*) CSQ2 knockdown in the RV as monitored by western blotting and (*B*) RV d*P*/d*t* as an indication of the contractile performance. (*C*) Tropomyosin, (*D*) troponin T, and (*E*) SERCA2a levels were monitored by western blotting in the RV homogenates. The symbol (*) denotes that the value is significantly different from the control value at $P < 0.05$ as determined by Student's *t*-test.

pulmonary artery banding is not sufficient to explain right heart failure,[13] the SU5416/hypoxia model provides a unique opportunity for studying RV failure. Further, as human RV pathology in PAH patients is not well defined, this animal model provides invaluable information.

This study, for the first time, followed a longer time course to observe changes in RV characteristics in this PAH model and found that RV decompensation is followed by the adaptation of the RV to sustain its contractility. RVSP was elevated to >70 mmHg at 5 weeks after the SU5416 injection and remained at this level for at least 12 weeks. Although the RV and lung weights were elevated after the SU5416/hypoxia treatment, no changes were noted in body weight or LV weight.

Bogaard *et al.*[13] reported that the administration of SU5416 and treatment with chronic hypoxia followed by the maintenance of rats in normoxia for 2 weeks promoted RV myocyte apoptosis and fibrosis. Increased myocardial fibrosis has also been reported to occur in the RV of rats exposed to SU5416/hypoxia.[19,20] In this study, we maintained rats in normoxia for 2, 5, and 14 weeks and found that both apoptosis and replacement fibrosis were increased. Increased apoptosis was associated with decreased GATA4 and increased p53 protein expression in the RV, following the SU5416/hypoxia treatment. These findings are consistent with the mechanism we reported previously, in which p53 negatively regulates GATA4 gene transcription by binding to the CBF/NF-Y transcription factor.[17] We employed p53 knock-out rats to directly show the role of p53 in SU5416/hypoxia-mediated RV myocyte apoptosis and found that, in the absence of p53, GATA4 downregulation, the induction of apoptosis, and the promotion of fibrosis were all attenuated. The reduced RV events were not due to the correction of PAH, as p53 knock-out rats had elevated RV pressure, consistent with the previous studies that have used p53-deficient mice[21] and rats injected with pifithrin-α to inhibit p53.[22] These results suggest that p53 inhibition may be a useful therapeutic approach to prevent RV decompensation in the setting of PAH, similar to the idea reported for LV failure.[9]

The major finding of the present study that was obtained unexpectedly is that despite the significant occurrence of RV myocyte death and replacement of RV myocytes with fibrotic regions, RV contractility remained strong. We initially hypothesized that RV deterioration would result in decreased RV contractility. Although RV pressure remained the same during the 5-, 8-, and 17-week time points after the SU5416 injection and RV myocyte apoptosis and fibrosis increased, d*P*/d*t* values increased as well. These results suggest that the remaining RV myocytes are capable of more superior contractile functions by becoming 'super RV myocytes'.

In this study, we present possible mechanisms by which super RV myocytes exhibit superior contractile functions. First, these myocytes seem to have higher levels of proteins involved in muscle contraction. We measured tropomyosin and troponin T and found that both proteins were elevated in the RV after SU5415/hypoxia treatment. The second mechanism involves the modulation of Ca^{2+} regulation, which is essential for muscle contraction. We found that exposure to

SU5416/hypoxia increased SERCA2a protein expression in the RV. SERCA2 regulates SR Ca^{2+} load, cytoplasmic Ca^{2+} removal, and the amount of Ca^{2+} available for cardiac contraction.[23] It is unlikely that increased SERCA2 reflects a general increase in the SR volume, as the expression levels of other SR proteins such as CSQ2 and triadin were decreased in super RV myocytes.

CSQ2 is the major Ca^{2+}-binding protein in the lumen of the SR[24,25]; however, its precise functions are not fully understood. As CSQ2 is downregulated in super RV myocytes, the reduction of this protein may be involved in the mechanism for improving RV contractility. Knocking down CSQ2 using an *in vivo* siRNA approach in rats resulted in markedly increased RV contractility as well as increased expressions of contractile and SR Ca^{2+} uptake proteins. Results from this study, which show that siRNA knockdown of CSQ2 increases the expression of SERCA2, are consistent with our previous observations that the SERCA2 expression is downregulated in transgenic mice overexpressing CSQ2.[26] Thus, downregulation of CSQ2 may be a way to increase cardiac contractility, and the super RV myocytes that remain in the decompensated RV may utilize this mechanism for adaptation.

One possible mechanism for CSQ2 to modulate the expression of contractile and SR Ca^{2+} uptake proteins is that CSQ2 directly regulates gene transcription. Calreticulin, the major Ca^{2+} binding protein of the non-striated muscle endoplasmic reticulum, has been shown to regulate gene transcription by interacting with the DNA-binding domain of the glucocorticoid receptor.[27] Thus, CSQ2 may also regulate both muscle contraction and gene transcription, perhaps in the structures such as nucleoplasmic reticulum[28] and perinuclear Ca^{2+} microdomain.[29] Further studies are needed to elucidate the mechanisms and functions of CSQ2 in regulating gene transcription.

In summary, by using the SU5416/hypoxia model of PAH and RV failure, the present study demonstrated that RV decompensation with the loss of a significant number of RV myocytes is followed by the adaptation of the remaining myocytes to perform superior contractile functions. This adaptation is achieved by forming super RV myocytes with increased contractile and SR Ca^{2+} uptake proteins. Longer time course studies are needed to define how adaptation may transition to maladaptation (see Supplementary material online, *Figure S4*), which may present key therapeutic targets to prevent RV failure. Although the occurrence of RV fibrosis in rats with PAH is consistent with human studies,[30–33] it is not yet known whether the apoptosis really occurs in the RV of PAH patients. The future studies of human PAH patients should also include the assessment of RV adaptation and maladaptation that are described in this study.

Supplementary material

Supplementary material is available at *Cardiovascular Research* online.

Conflict of interest: none declared.

Funding

This work was supported in part by National Institutes of Health (R01HL72844) to Y.J.S.

References

1. Galiè N, Hoeper MM, Humbert M, Torbicki A, Vachiery JL, Barbera JA, Beghetti M, Corris P, Gaine S, Gibbs JS, Gomez-Sanchez MA, Jondeau G, Klepetko W, Opitz C, Peacock A, Rubin L, Zellweger M, Simonneau G; ESC Committee for Practice Guidelines (CPG). Guidelines for the diagnosis and treatment of pulmonary hypertension: the Task Force for the Diagnosis and Treatment of Pulmonary Hypertension of the European Society of Cardiology (ESC) and the European Respiratory Society (ERS), endorsed by the International Society of Heart and Lung Transplantation (ISHLT). *Eur Heart J* 2009;**30**:2493–2537.
2. Benza RL, Miller DP, Frost A, Barst RJ, Krichman AM, McGoon MD. Analysis of the lung allocation score estimation of risk of death in patients with pulmonary arterial hypertension using data from the REVEAL Registry. *Transplantation* 2010;**90**:298–305.
3. Humbert M, Sitbon O, Yaïci A, Montani D, O'Callaghan DS, Jaïs X, Parent F, Savale L, Natali D, Günther S, Chaouat A, Chabot F, Cordier JF, Habib G, Gressin V, Jing ZC, Souza R, Simonneau G; French Pulmonary Arterial Hypertension Network. Survival in incident and prevalent cohorts of patients with pulmonary arterial hypertension. *Eur Respir J* 2010;**36**:549–555.
4. Thenappan T, Shah SJ, Rich S, Tian L, Archer SL, Gomberg-Maitland M. Survival in pulmonary arterial hypertension: a reappraisal of the NIH risk stratification equation. *Eur Respir J* 2010;**35**:1079–1087.
5. Delcroix M, Naeije R. Optimising the management of pulmonary arterial hypertension patients: emergency treatments. *Eur Respir Rev* 2010;**19**:204–211.
6. Boxt LM. Radiology of the right ventricle. *Radiol Clin North Am* 1999;**37**:379–400.
7. Budev MM, Arroliga AC, Wiedemann HP, Matthay RA. Cor pulmonale: an overview. *Semin Respir Crit Care Med* 2003;**24**:233–244.
8. Voelkel NF, Quaife RA, Leinwand LA, Barst RJ, McGoon MD, Meldrum DR, Dupuis J, Long CS, Rubin LJ, Smark FW, Suzuki YJ, Gladwin M, Denholm EM, Gail DB. Right ventricular function and failure: the need to know more. Report of a National Heart, Lung and Blood Institute Working Group on Cellular and Molecular Mechanisms of Right Heart Failure. *Circulation* 2006;**114**:1883–1891.
9. Sano M, Minamino T, Toko H, Miyauchi H, Orimo M, Qin Y, Akazawa H, Tateno K, Kayama Y, Harada M, Shimizu I, Asahara T, Hamada H, Tomita S, Molkentin JD, Zou Y, Komuro I. p53-induced inhibition of Hif-1 causes cardiac dysfunction during pressure overload. *Nature* 2007;**446**:444–448.
10. Gómez A, Bialostozky D, Zajarias A, Santos E, Palomar A, Martínez ML, Sandoval J. Right ventricular ischemia in patients with primary pulmonary hypertension. *J Am Coll Cardiol* 2001;**38**:1137–1142.
11. Abe K, Toba M, Alzoubi A, Ito M, Fagan KA, Cool CD, Voelkel NF, McMurtry IF, Oka M. Formation of plexiform lesions in experimental severe pulmonary arterial hypertension. *Circulation* 2010;**121**:2747–2754.
12. Taraseviciene-Stewart L1, Kasahara Y, Alger L, Hirth P, Mc Mahon G, Waltenberger J, Voelkel NF, Tuder RM. Inhibition of the VEGF receptor 2 combined with chronic hypoxia causes cell death-dependent pulmonary endothelial cell proliferation and severe pulmonary hypertension. *FASEB J* 2001;**15**:427–438.
13. Bogaard HJ, Natarajan R, Henderson SC, Long CS, Kraskauskas D, Smithson L, Ockaili R, McCord JM, Voelkel NF. Chronic pulmonary artery pressure elevation is insufficient to explain right heart failure. *Circulation* 2009;**120**:1951–1960.
14. Park AM, Wong CM, Jelinkova L, Liu L, Nagase H, Suzuki YJ. Pulmonary hypertension-induced GATA4 activation in the right ventricle. *Hypertension* 2010;**56**:1145–1151.
15. Park AM, Suzuki YJ. Effects of intermittent hypoxia on oxidative stress-induced myocardial damage in mice. *J Appl Physiol* 2007;**102**:1806–1814.
16. Kitta K, Day RM, Kim Y, Torregroza I, Evans T, Suzuki YJ. Hepatocyte growth factor induces GATA-4 phosphorylation and cell survival in cardiac muscle cells. *J Biol Chem* 2003;**278**:4705–4712.
17. Park AM, Nagase H, Liu L, Vinod Kumar S, Szwergold N, Wong CM, Suzuki YJ. Mechanism of anthracycline-mediated down-regulation of GATA4 in the heart. *Cardiovasc Res* 2011;**90**:97–104.
18. Costello CM, Howell K, Cahill E, McBryan J, Konigshoff M, Eickelberg O, Gaine S, Martin F, McLoughlin P. Lung-selective gene responses to alveolar hypoxia: potential role for the bone morphogenetic antagonist gremlin in pulmonary hypertension. *Am J Physiol Lung Cell Mol Physiol* 2008;**295**:L272–L284.
19. Alzoubi A, Toba M, Abe K, O'Neill KD, Rocic P, Fagan KA, McMurtry IF, Oka M. Dehydroepiandrosterone restores right ventricular structure and function in rats with severe pulmonary arterial hypertension. *Am J Physiol Heart Circ Physiol* 2013;**304**:H1708–H1718.
20. Drake JI, Bogaard HJ, Mizuno S, Clifton B, Xie B, Gao Y, Dumur CI, Fawcett P, Voelkel NF, Natarajan R. Molecular signature of a right heart failure. *Am J Respir Cell Mol Biol* 2011;**45**:1239–1247.
21. Mizuno S, Bogaard HJ, Kraskauskas D, Alhussaini A, Gomez-Arroyo J, Voelkel NF, Ishizaki T. p53 Gene deficiency promotes hypoxia-induced pulmonary hypertension and vascular remodeling in mice. *Am J Physiol Lung Cell Mol Physiol* 2011;**300**:L753–L761.
22. Jacquin S, Rincheval V, Mignotte B, Richard S, Humbert M, Mercier O, Londoño-Vallejo A, Fadel E, Eddahibi S. Inactivation of p53 is sufficient to induce development of pulmonary hypertension in rats. *PLoS ONE* 2015;**10**:e0131940.
23. Periasamy M, Huke S. SERCA pump level is a critical determinant of Ca^{2+} homeostasis and cardiac contractility. *J Mol Cell Cardiol* 2001;**33**:1053–1063.
24. Jones LR, Suzuki YJ, Wang W, Kobayashi YM, Ramesh V, Franzini-Armstrong C, Cleemann L, Morad M. Regulation of Ca^{2+} signaling in transgenic mouse cardiac myocytes overexpressing calsequestrin. *J Clin Invest* 1998;**101**:1385–1393.
25. Knollmann BC. New roles of calsequestrin and triadin in cardiac muscle. *J Physiol* 2009;**587**:3081–3087.
26. Ihara Y, Suzuki YJ, Kitta K, Jones LR, Ikeda T. Modulation of gene expression in transgenic mouse hearts overexpressing calsequestrin. *Cell Calcium* 2002;**32**:21–29.

27. Burns K, Duggan B, Atkinson EA, Famulski KS, Nemer M, Bleackley RC, Michalak M. Modulation of gene expression by calreticulin binding to the glucocorticoid receptor. *Nature* 1994;**367**:476–480.
28. Echevarría W, Leite MF, Guerra MT, Zipfel WR, Nathanson MH. Regulation of calcium signals in the nucleus by a nucleoplasmic reticulum. *Nat Cell Biol* 2003;**5**:440–446.
29. Guo A, Cala SE, Song LS. Calsequestrin accumulation in rough endoplasmic reticulum promotes perinuclear Ca^{2+} release. *J Biol Chem* 2012;**287**:16670–16680.
30. Overbeek MJ, Mouchaers KT, Niessen HM, Hadi AM, Kupreishvili K, Boonstra A, Voskuyl AE, Belien JA, Smit EF, Dijkmans BC, Vonk-Noordegraaf A, Grünberg K. Characteristics of interstitial fibrosis and inflammatory cell infiltration in right ventricles of systemic sclerosis-associated pulmonary arterial hypertension. *Int J Rheumatol* 2010; **2010**:604615.
31. Bessa LG, Junqueira FP, Bandeira ML, Garcia MI, Xavier SS, Lavall G, Torres D, Waetge D. Pulmonary arterial hypertension: use of delayed contrast-enhanced cardiovascular magnetic resonance in risk assessment. *Arq Bras Cardiol* 2013;**101**: 336–343.
32. Ozawa K, Funabashi N, Kataoka A, Tanabe N, Yanagawa N, Tatsumi K, Kobayashi Y. Myocardial fibrosis in the right ventricle detected on ECG gated 320 slice CT showed a short term poor prognosis in subjects with pulmonary hypertension. *Int J Cardiol* 2013; **168**:584–586.
33. Ozawa K, Funabashi N, Tanabe N, Tatsumi K, Yanagawa N, Kataoka A, Kobayashi Y. Two dimensional global longitudinal strain of right ventricle using transthoracic echocardiography can detect right ventricular fibrosis confirmed by 320 slice CT in pulmonary hypertension. *Int J Cardiol* 2014;**172**:e230–e233.